JAAS

ROYAL SOCIETY OF CHEMISTRY

PAPER

View Article Online
View Journal | View Issue

Check for updates

Cite this: J. Anal. At. Spectrom., 2026, 41, 333

Detection and quantification of trace technetium in the presence of molybdenum using laser-induced breakdown spectroscopy

Hunter B. Andrews, *[a] Zachary Murphy, [c] Mauro Martinez, [bf] John Lucchi, [b] Vasileios Anagnostopoulos [c] and Matthieu Baudelet *[bcde]

Technetium (Tc) is a very important element that is encountered in many aspects, from its presence in radioactive waste and its potential environmental impact to its use as a medical radioisotope. Its detection and quantification in liquid samples is traditionally cumbersome, involving detailed sample preparation and analysis by mass spectrometry or scintillation. This article demonstrates the first comprehensive emission spectral analysis of Tc from a liquid sample by immobilization in a polymer and analysis by laser-induced breakdown spectroscopy (LIBS). A survey of LIBS spectra was completed to identify the strongest analytical lines for quantification of trace Tc in the presence of Mo. The quantification of Tc in a Mo-containing matrix was selected because Tc radioisotopes are the daughter products of Mo isotope decay. The first reported calibration curves by LIBS are provided with limits of detection and quantification down to 0.710 μg mL^{-1} and 1.39 μg mL^{-1}, respectively. Ultimately, this study demonstrated the feasibility of trace Tc quantification using LIBS and will serve as a reference for future research related to monitoring this radioactive species.

Received 20th August 2025
Accepted 17th November 2025

DOI: 10.1039/d5ja00319a

rsc.li/jaas

Open Access Article. Published on 18 November 2025. Downloaded on 5/24/2026 6:58:57 PM. This article is licensed under a Creative Commons Attribution-NonCommercial 3.0 Unported Licence.

1. Introduction

Advanced nuclear reactor designs are being heavily researched to meet growing energy demands. One advanced reactor design, the molten salt reactor (MSR), stands apart from the rest because it uses nuclear fuel dissolved into a high-temperature molten salt.[1,2] This dissolved liquid fuel circulates through the primary fuel circuit, where fission occurs in the core, and then the resultant fission products decay as the molten salt passes through a heat exchanger before reentering the core. This dissolved fuel form results in high efficiency and passive safety features, but the transient fission process results in a diverse inventory of fission products within the salt. Volatile species, noble gases, and aerosolized salt will evolve into the headspace, where they must be treated in the off-gas system to prevent unintentional release to the environment.[3] Similarly, other isotopes may be targeted for extraction from the molten salt for a variety of applications. One such example is molybdenum-99 (^{99}Mo), an isotope continually produced in nuclear fission which decays into the metastable technetium-99m (^{99m}Tc). Technetium-99m has a half-life of 6.01 h and is used for medical imaging. Several investigations have proposed harvesting ^{99}Mo as a source of ^{99m}Tc from MSRs as a potential replacement for current generation methods.[4,5]

The most abundant isotope of Tc, ^{99}Tc, has a half-life of 2.13×10^5 years, and it is one of the most important radionuclides for assessing the safety of environmental radioactivity and radioactive waste management.[6,7] When Tc is exposed to the atmosphere or any moderately oxidizing environment, it is found in the form of pertechnetate (TcO_4^-). Pertechnetate is highly soluble, does not sorb onto sediments, and migrates at the same velocity as groundwater.[8] Under reducing conditions, Tc is found in the +4 valence state: it hydrolyzes in the presence of water but is encountered as sparingly soluble TcO_2 in the absence of water.[9] Furthermore, in the +4 oxidation state, Tc has been reported to complex with ligands such as carbonates, citrate, and natural organic matter.[10–12]

Because of its very low environmental concentration, the sample preparation, preconcentration, and chemical separation for removal of interferences are crucial steps for accurately determining ^{99}Tc concentrations in environmental samples. Several methods have been used in the past to determine ^{99}Tc in aqueous samples: gas flow with Geiger–Müller counter after anion exchange pretreatment in seawater,[13] proportional counting after solvent extraction in radioactive waste,[14] inductively coupled plasma mass spectrometry (ICP-MS) for water samples

[a]Radioisotope Science and Technology Division, Oak Ridge National Laboratory, Oak Ridge, Tennessee, USA. E-mail: andrewshb@ornl.gov
[b]National Center for Forensic Science, University of Central Florida, Orlando, Florida, USA. E-mail: baudelet@ucf.edu
[c]Chemistry Department, University of Central Florida, Orlando, Florida, USA
[d]CREOL—The College of Optics and Photonics, University of Central Florida, Orlando, Florida, USA
[e]Anthropology Department, University of Central Florida, Orlando, Florida, USA
[f]Now at Department of Environmental Medicine and Public Health, Icahn School of Medicine at Mount Sinai, New York, New York, USA

Open Access Article. Published on 18 November 2025. Downloaded on 5/24/2026 6:58:57 PM. This article is licensed under a Creative Commons Attribution-NonCommercial 3.0 Unported Licence.

after solid-phase extraction,[15–17] accelerated mass spectroscopy in seawater,[18] and a sequential injection separation system in conjunction with liquid scintillation counting for tank waste samples.[19] Thus, the goal of this study was to investigate the detection and quantification of trace ^{99}Tc using laser-induced breakdown spectroscopy (LIBS) as an alternative analytical technique. LIBS is a powerful technique increasingly being applied in the nuclear field because of its versatility in application and sensitivity.[20] LIBS has been investigated in many situations for in-field environmental sampling and is being developed as an online monitoring tool for MSRs and thus the potential quantification of Tc could be extended to these monitoring applications.[21] Furthermore, LIBS requires minimal sample preparation compared with other analytical techniques.

LIBS is recognized as a rapid and sensitive technique that generally provides elemental analysis at levels of parts per million in most substrates.[22] Although several studies have mentioned the potential application of LIBS to detecting Tc,[23–25] Tc has not been extensively studied by LIBS, and most studies relied on using surrogate species. To the best of the authors' knowledge, only one previous literature study by Samek *et al.* reported three Tc LIBS emissions from a single 1000 μg mL^{-1} sample during the analysis of liquid samples.[26] In this study by Samek *et al.* the detection limit of Tc was estimated to be 25 mg L^{-1} using a single point response.

Thus, this article provides a full demonstration of Tc emission spectroscopy by LIBS and its quantification at trace concentrations (*i.e.*, <1000 μg mL^{-1}) in an aqueous solution after immobilization in a polyvinyl alcohol (PVA) film. Additionally, the calibration system that was investigated included Mo at competing concentrations to examine the feasibility of monitoring Tc concentrations in a nuclear system containing the parent isotope Mo, such as an MSR. A comprehensive emission peak survey under concentrated and trace concentrations was performed to provide a knowledge base for future Tc LIBS studies.

2. Experimental

2.1 Tc standards preparation

The ^{99}Tc samples were prepared using a 0.02 mCi mL^{-1} (1.17 mg mL^{-1}) solution of NH_4TcO_4 in water (Eckert and Ziegler, Valencia, California, USA), PVA (98–99% hydrolyzed, Thermo Scientific, USA), a 1000 μg mL^{-1} Mo ICP-MS standard (PlasmaCAL, Analytichem, Canada) and ultrapure water (18.2 MΩ cm; Barnstead, Thermo Electronics, USA). An aqueous calibration curve was initially prepared with Tc concentrations ranging from 0 to 100 μg mL^{-1}, each containing 50 μg mL^{-1} Mo. Generally, Mo was included in the study due to its relevance to Tc detection and to understand which Tc peaks used for regression either had or didn't have interferences with Mo. This Mo concentration was selected to be in the middle of the Tc calibration range. Direct laser ablation of liquids is difficult to perform due to splashing, plasma quenching, and laser focal point issues, these aqueous samples were transformed into solid samples. This was completed by preparing samples in 2% m/v PVA matrices, similar to the method proposed by Lin *et al.*[27] A diagram of the procedure used is shown in Fig. S1. This method allows the solutions to be converted into a solid matrix for testing thereby mitigating the challenges associated with liquid samples. To convert to the solid matrix, 250 μL of each solution was deposited into a mold and dried to form a thin film. The films were nominally 5 mg in mass and had a diameter of 8 mm and thickness of 20 μm. These films were then mounted on microscope slides with double-sided Cu tape for analysis. Care was taken that no Cu was seen in the recorded spectra, indicating only the PVA thin film was ablated. The PVA solid sample conversion resulted in an approximately 50× preconcentration of the analytes, making it an ideal approach for analyzing trace species in aqueous samples using LIBS by enhancing the number of Tc atoms within the plasma. A list of the emission survey and calibration samples is shown in Table 1 with their nominal, measured solution, and measured film concentrations. The concentrations of Tc and Mo were standardized with liquid scintillation counting and ICP-MS, respectively. To analyze the thin films with these methods, they were digested in 2% HNO_3 with mild heating and sonication before analysis. With the goal of analyzing quantification capabilities for aqueous samples using this preparation method, the measured solution values were used throughout this study.

2.2 Instrumentation

LIBS data were acquired using a J200 LIBS system (Applied Spectra Inc., West Sacramento, California, USA). In this study,

Table 1 Sample set concentrations

Nominal solution (μg mL^{-1})		Measured solution (μg mL^{-1})		Measured film (μg g^{-1})	
Mo	Tc	Mo	Tc	Mo	Tc
0	0	—	—	—	—
50	0	41.8 ± 0.2	—	2223.6 ± 217.3	—
0	50	—	54.79 ± 1.81	—	2288.0 ± 92.7
50	1	48.5 ± 2.8	1.42 ± 0.06	2461.7 ± 211.6	54.0 ± 4.2
50	5	49.0 ± 0.7	5.84 ± 0.21	2212.8 ± 110.3	232.7 ± 19.5
50	10	49.2 ± 2.7	11.53 ± 0.72	2335.1 ± 242.5	466.5 ± 17.3
50	25	46.9 ± 1.9	28.22 ± 1.23	2087.0 ± 177.7	1162.5 ± 58.7
50	50	48.6 ± 3.9	53.96 ± 2.06	2247.9 ± 106.9	2337.0 ± 93.1
50	100	48.8 ± 1.6	106.78 ± 2.86	2160.4 ± 159.4	4542.6 ± 169.4

 This journal is © The Royal Society of Chemistry 2026

Open Access Article. Published on 18 November 2025. Downloaded on 5/24/2026 6:58:57 PM. This article is licensed under a Creative Commons Attribution-NonCommercial 3.0 Unported Licence.

the instrument consisted of a 266 nm Nd:YAG laser (8 ns, 10 Hz) with an energy of 13 mJ, and two spectrometers were used: (1) a multichannel spectrometer for broad spectral coverage and (2) a Czerny–Turner (CZ) spectrometer equipped with an intensified CCD (ICCD) detector for better sensitivity for quantitative analysis. For the CZ spectrometer, a 0.5 μs gate delay and a 3 μs exposure time was used. The broadband multichannel spectrometer was set at 1.0 μs delay and a fixed duration of 1 ms, which is essentially infinite relative to the plasma lifetime. Two spectral emission surveys were conducted with the CZ spectrometer, both using a grating with 2400 lines per millimeter and scanning between 200 and 800 nm. The first was conducted on an NH_4TcO_4 solution dried on a Si wafer, providing direct laser ablation of NH_4TcO_4 salt. The second was conducted on the PVA film containing only Tc. Each survey spectrum is the accumulation of 23 shots, equated to one line scan along the sample.

An Ar background atmosphere (flow of 1 L min^{-1}) was employed to avoid interaction with N and O in the air. The Tc and Mo in PVA films were analyzed to build calibration curves using a 100 μm spot size, accumulating spectra created while moving the sample at a speed of 1000 μm s^{-1} over a 5 mm line (*e.g.*, 50 shots per line, no overlap between shots). In total, 30 lines were performed per sample. CZ spectrometer calibration spectra were collected with a grating with 2400 lines per millimeter. Data processing was performed using MATLAB (R2015a, MathWorks), Origin (2022 SR1, OriginLab Corporation), and Python 3.

3. Results and discussion

3.1 Tc emission line survey

First, a concentrated NH_4TcO_4 solution dried on a Si wafer was used to provide a thorough investigation of emissions of Tc using LIBS. This was the first thorough emission survey of Tc using LIBS. The results were compared with previous arc and spark[28] spectral records and are summarized in the SI for the reader's reference. For a more relevant emission survey for this analytical study, a blank sample, a 50 μg mL^{-1} Mo sample, and a 50 μg mL^{-1} Tc sample were each scanned from 200 to 800 nm with the CZ spectrometer and using a grating with 2400 lines per millimeter to investigate the lines of interest for this study (*i.e.* at trace concentrations). The top five neutral and ionized emissions based on relative emission intensity are detailed in Table 2, along with their relevant transition properties (A), energy levels (E), and degeneracies (g).[29] Additionally, selected spectral windows highlighting these peaks, along with the blank and Mo sample spectra, are shown in Fig. 1. A more in-depth investigation, as well as arc and spark peak locations, is provided in the SI.

The strongest Tc emission peak is the singly-ionized peak at 254.32 nm. The two nearby Tc II peaks also exhibit strong emissions, scaling in accordance with their degeneracy-weighed transition probability (gA) factors. The two remaining Tc II emission lines provide weaker emissions and are in regions that have Mo emissions. As for Tc I lines, the 363.61 and 403.16 nm emissions are the strongest and are on par with the strongest ionized emissions. These strong lines may be preferred over Tc II lines for quantification because of the decreased effect of electron density and self-absorption on neutral emission lines. Although this emission survey was performed with the higher-sensitivity CZ spectrometer, these strong emissions were all observed in the broadband multichannel spectrometer, but the signal-to-noise levels were lower. This result has implications for monitoring Tc in less-tailored LIBS devices for online monitoring in nuclear applications.

3.2 Quantification of trace Tc

Based on the identified strong emission peaks in the survey, calibration curves were developed with the broadband multichannel spectrometer and the CZ ICCD spectrometer. The calibration sample set (Table 1) was used where the Tc concentration in solution before immobilization ranged from 0 to 100 μg mL^{-1}, and the Mo concentration was held constant at 50 μg mL^{-1}. For each sample, 30 lines of 50 shots were collected. Each line was accumulated into a single spectrum for analysis with a better signal-to-noise ratio. Peak areas were integrated using Simpson's rule and then background corrected. Peak areas were used rather than peak intensities due to their increased robustness to the influence of peak broadening, asymmetry, and noise. Because the concentration of the

Table 2 Identified strongest ionized and neutral emission lines for Tc detection at trace levels[a]

Ion	Wavelength (nm)	Relative intensity	A (10^8 s^{-1})	E_{low} (eV)	E_{high} (eV)	g_{low}	g_{high}
II	254.32	1.00	4.10	0.000000	4.873618	7	9
II	260.99	0.88	3.80	0.000000	4.748942	7	7
II	264.70	0.59	3.70	0.000000	4.682537	7	5
II	321.20	0.38	1.90	1.564333	5.423234	5	5
II	323.70	0.53	1.90	1.564333	5.393432	5	7
I	363.61	0.91	1.57	0.318998	3.727869	10	12
I	371.89	0.51	1.05	0.403061	3.736048	8	10
I	403.16	0.88	1.01	0.318998	3.393421	10	10
I	426.22	0.52	0.40	0.000000	2.908075	6	6
I	429.70	0.76	0.42	0.000000	2.884532	6	8

[a] Relative intensity is the background corrected intensity relative to the strongest Tc peak.

Open Access Article. Published on 18 November 2025. Downloaded on 5/24/2026 6:58:57 PM.
This article is licensed under a Creative Commons Attribution-NonCommercial 3.0 Unported Licence.

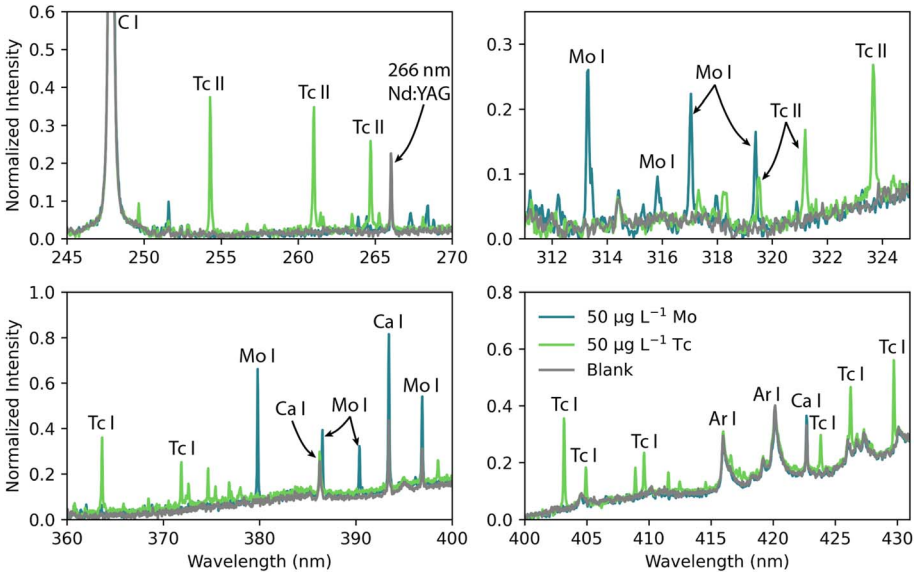

Fig. 1 Identified strong emissions for Tc in trace conditions. Spectra for a blank sample and nominally 50 µg mL^{-1} Mo. Each subplot shows different wavelength windows from the same spectra.

calibration ranged greater than an order of magnitude, a weighted regression was used in which the weight was inversely proportional to the variance of the data. This method was recommended in several literature studies when the variance scaled with concentration.[30,31] The limits of detection (LODs) and limits of quantification (LOQs) were determined using the 95% prediction intervals of the linear model, as described by Mermet.[30,31] Here, the LOD is defined as the concentration value where the upper level of the 95% prediction band at the blank intercepts with the regression fit. This statistically relates to the concentration that can be detected from the blank with 95% confidence. Similarly, the LOQ is defined as concentration value where the lower level of the prediction interval is equal to the upper level of the 95% prediction band at the blank. This statistically relates to the concentration that can be quantified above the blank with 95% confidence.

The figures of merit for the multichannel calibration models for Tc peaks with >0.75 relative intensity (see Table 2) are detailed in Table 3. All peaks provided calibration curves with R^2 > 0.99 and LODs < 10 µg mL^{-1}. These figures of merit offer promise for monitoring Tc using a multichannel spectrometer to monitor nuclear streams, such as the effluent of an MSR. Most MSR LIBS work has focused on using multichannel spectrometers because of their reduced footprint, broadband coverage, and robustness for deployed systems.[32] The calibration curve for 429.70 nm is shown in Fig. 2; the other multichannel spectrometer calibration plots are provided in the SI.

In addition to the broadband calibration, two spectral windows identified from the emission survey were selected for further investigation of Tc quantification using the CZ ICCD spectrometer. The first window, centered at 397 nm, contained several strong, neutral Tc peaks (398.49, 403.16, and 404.91 nm) without any interreferences from Mo. The second window, centered at 319 nm, contained weaker, singly ionized Tc peaks (319.52, 321.20, 323.70, and 328.20 nm), as well as an interference from the neutral 319.39 nm Mo I resonance peak. Portions of the collected spectral windows are shown in Fig. 3 as a function of Tc concentration.

The broadband spectra and CZ ICCD spectra were checked for correlated signals (outside of Mo or Tc) to identify

Table 3 Summary of multichannel univariate calibration model figures of merit

Emission peak	Concentration range (µg mL^{-1})	R^2	LOD (µg mL^{-1})	LOQ (µg mL^{-1})
254.32 nm Tc II	<100	0.9940	5.97	11.9
260.99 nm Tc II	<100	0.9934	6.84	13.6
363.61 nm Tc I	<100	0.9937	6.88	13.5
403.16 nm Tc I	<100	0.9945	6.73	13.2
429.70 nm Tc I	<100	0.9983	4.45	8.80

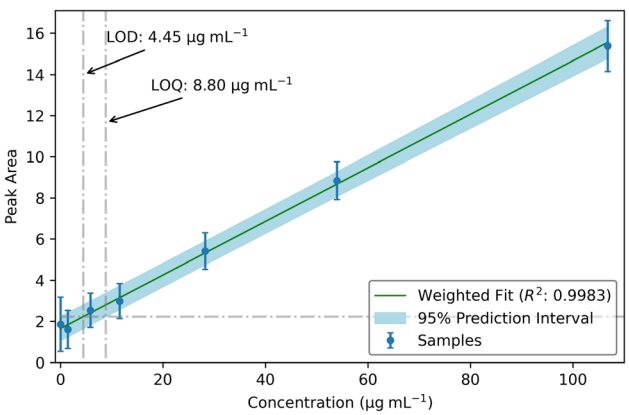

Fig. 2 Tc calibration curve based on the 429.70 nm emission peak from the multichannel spectrometer.

 This journal is © The Royal Society of Chemistry 2026

Open Access Article. Published on 18 November 2025. Downloaded on 5/24/2026 6:58:57 PM.
This article is licensed under a Creative Commons Attribution-NonCommercial 3.0 Unported Licence.

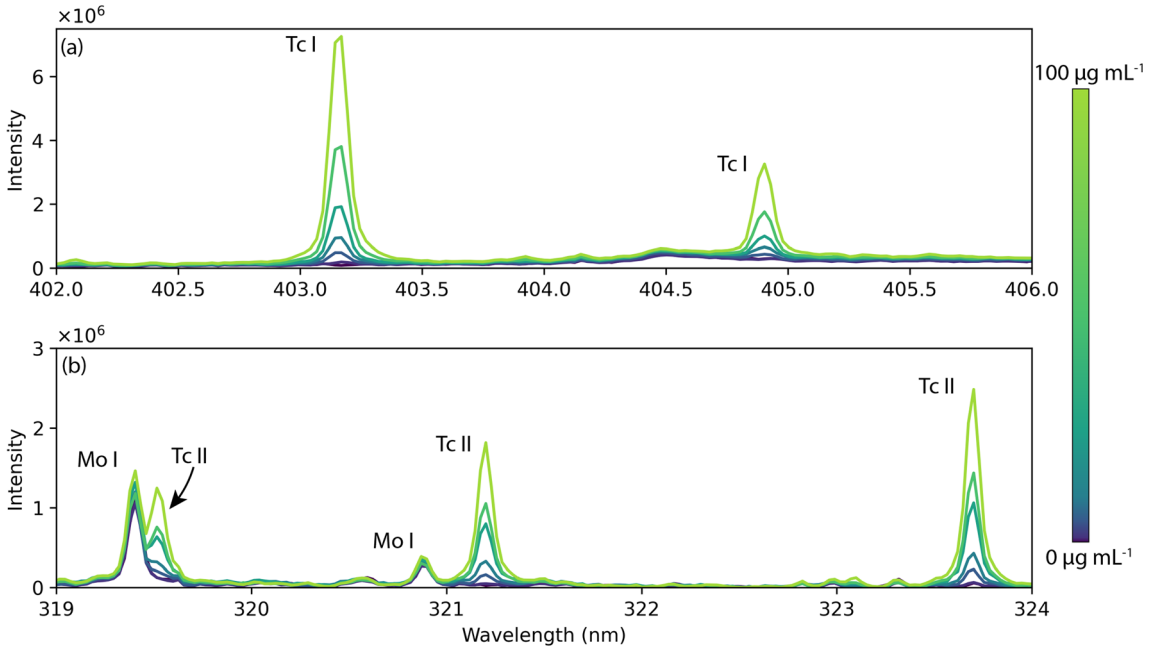

Fig. 3 LIBS spectra as a function of Tc concentration collected on the CZ ICCD spectrometer. Two spectral windows were selected because of their (a) strong neutral emissions and (b) weak ionized emissions with Mo interferences.

Table 4 Summary of CZ ICCD univariate calibration model figures of merit

Emission peak	Concentration range (µg mL^{-1})	R^2	LOD (µg mL^{-1})	LOQ (µg mL^{-1})
398.49 nm Tc I	<100	0.9929	2.77	5.26
403.16 nm Tc I	<100	0.9986	0.710	1.39
404.91 nm Tc I	<100	0.9895	4.32	8.14
[a]319.52 nm Tc II	<25	0.9828	6.51	12.7
321.20 nm Tc II	<25	0.9980	2.19	4.29
323.70 nm Tc II	<25	0.9982	2.10	4.12
328.20 nm Tc II	<25	0.9834	6.39	12.5

[a] Model developed using curve fitting.

a normalization technique, although none proved viable over a standard background correction. A calibration model was developed for each peak, along with the corresponding LOD and LOQ. A summary of these univariate calibrations is provided in Table 4.

The univariate calibration model for the Tc I 403.16 nm emission proved to be the best. A plot of this model is shown in Fig. 4, highlighting its linearity across the concentration range. Because this peak has strong emission, detection in the range of parts per billion is possible with a LOD of 0.710 µg mL^{-1}. This peak was also used for a multichannel spectrometer calibration; thus, the improvement in detection performance is estimated to be a factor of approximately 8.5 when using the ICCD-equipped spectrometer. The other neutral Tc peaks in this window also

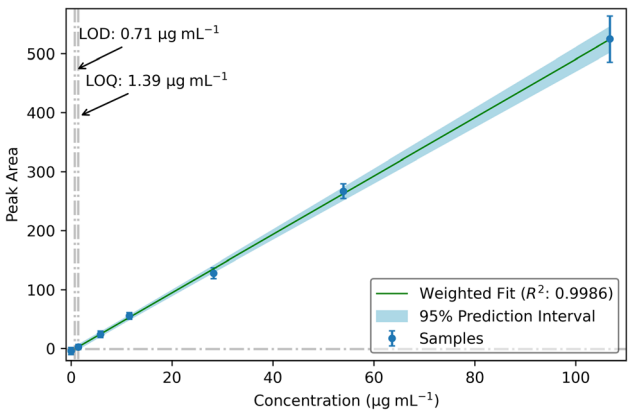

Fig. 4 Tc I 403.16 nm emission signal from LIBS collected using the CZ ICCD spectrometer as a function of Tc concentration. The error bars correspond to 2× standard error (n = 60).

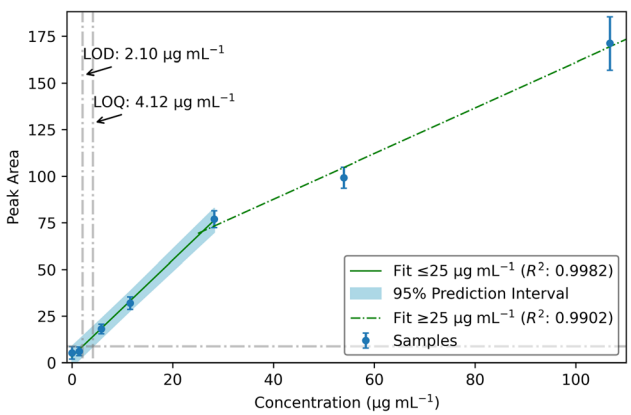

Fig. 5 Self-absorption behavior of the 323.70 nm Tc II emission peak collected on the CZ ICCD spectrometer *versus* concentration. Note that error bars correspond to 2× standard error (n = 60).

Open Access Article. Published on 18 November 2025. Downloaded on 5/24/2026 6:58:57 PM.
This article is licensed under a Creative Commons Attribution-NonCommercial 3.0 Unported Licence.

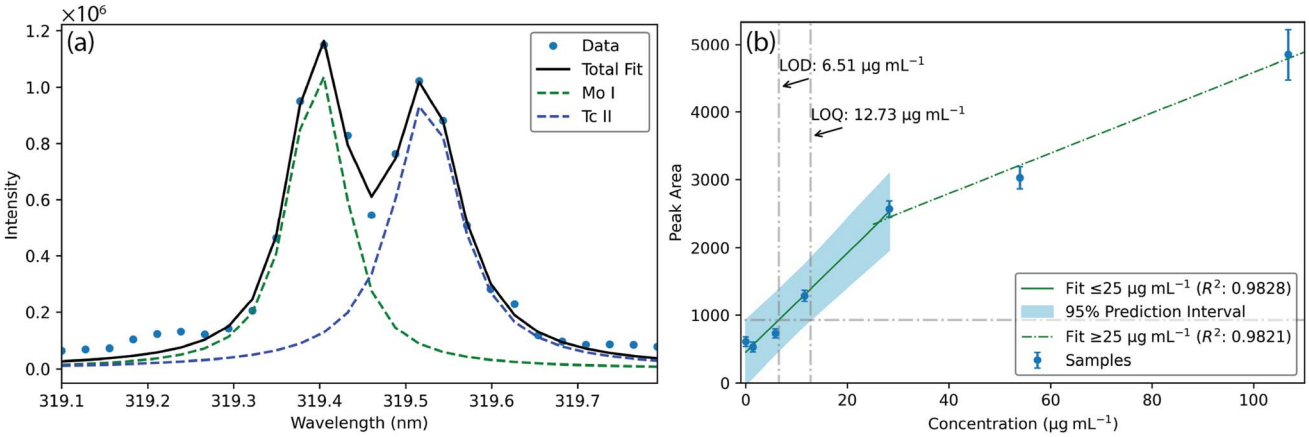

Fig. 6 (a) Peak fitting of Mo and Tc emissions at 319 nm and (b) corresponding calibration model. The error bars in (b) correspond to 2× standard error ($n = 60$).

perform well, although with slightly reduced qualities of fit. Calibration model plots are provided for the remaining lines in the SI.

The ionized Tc emissions exhibited signs of self-absorption. This behavior is shown in Fig. 5, in which the emission area *versus* concentration trend bends from one linear regime to another reduced slope around 25 μg mL^{-1}. Self-absorption is the result of emitted photons being absorbed by atoms within the plasma itself. As the concentration of the analyte grows, the number of atoms within the plasma capable of absorbing these photons grows in turn. This phenomenon is especially true early in the plasma lifetime, when ionized species are more dominant, which is why this behavior affects the singly ionized emissions and the neutral lines appear unaffected in this concentration range (*i.e.* 25–100 μg mL^{-1}).[22] Interestingly, this behavior is not shown in the ionized line calibrations using the multichannel spectrometer. This may be a result of the lower resolving power and/or the optical configuration of the broadband spectrometer, which uses a fiber bundle.

This nonlinear behavior can be fit using second-order polynomials or using a log–log transformation with a linear fit. However, for this study, the detection and quantification at trace concentrations were the focus; therefore, only the lower linear regimes were fit to estimate the detection limits of singly ionized emissions. The figures of merit of these calibration models are provided in Table 3, and individual calibration plots are provided in the SI. The 323.70 nm Tc II line provides the best fit and detection limits for the ionized peaks that were examined. The other 321.20 nm ionized peak demonstrates detection capabilities similar to the neutral lines, albeit at a far-reduced concentration range.

The presence of Mo shown in the neutral Mo 319.39 nm emission significantly interfered with the singly ionized Tc emission peak at 319.52 nm. To develop a univariate model using this peak, separation of the two peaks was required. This separation was done by fitting two Voigt profiles to the known emission wavelength centers using the 50 μg mL^{-1} Mo and 100 μg mL^{-1} Tc sample spectra. The two fitted peaks, as well as their sum, are shown in Fig. 6a compared with the measured spectrum. These peaks were then scaled to each sample's spectrum using a least squares fit. The scaled fits for 319.52 nm Tc II were then integrated to form a calibration model similar to those previously described (Fig. 6b).

Again, the singly ionized emission showed self-absorption behavior, resulting in only concentrations nominally <25 μg mL^{-1} Tc being regressed to assess detection limits. As expected for an interfered peak, the fit was slightly weaker, with an R^2 of 0.9828, and the detection limits were elevated to 6.51 μg mL^{-1} Tc. However, many scenarios with emission peaks will likely have interferences and the ability to detect Tc at low micrograms-per-milliliter levels through deconvolution, which is significant for the prospect of monitoring sample streams using LIBS.

4. Conclusions

This article discusses the emission spectroscopy of ^{99}Tc in aqueous solutions after immobilization in PVA films and analysis by LIBS. Given the scarce information on LIBS signatures of Tc in literature, this study serves as foundational knowledge for the emission profiles of Tc in LIBS measurements by providing emission line surveys under different conditions. Additionally, calibration models and their respective figures of merit for several peaks and different spectrometers provided serve as a reference for future researchers perusing the quantification of Tc using LIBS for various applications.

Successful quantification of trace Tc in a Mo-containing matrix was achieved with both broadband and narrowband spectrometers, with LODs down to 0.710 μg mL^{-1} in aqueous samples. The presence of Mo is expected in reactor conditions when monitoring Tc concentrations and would act as a potential source of interfering peaks. Fortunately, in this study it was not detrimental for Tc analysis thanks to fitting of the emission peaks and the appropriate choice of spectral ranges for analysis and calibration models. However, further studies are needed on Tc determination in more complex matrices, such as geological and mineral samples to simulate environmental contamination and molten salt matrices.

 This journal is © The Royal Society of Chemistry 2026

Open Access Article. Published on 18 November 2025. Downloaded on 5/24/2026 6:58:57 PM. This article is licensed under a Creative Commons Attribution-NonCommercial 3.0 Unported Licence.

Author contributions

Conceptualization (H. B. A., M. B., V. A.), Data curation (H. B. A., M. M., Z. M., J. L., M. B.), formal analysis (H. B. A., M. B.), funding acquisition (H. B. A., M. B.), investigation (H. B. A., M. B.), methodology (H. B. A., M. B.), visualization (H. B. A., M. B.), writing – original draft (H. B. A., M. B.), writing – review & editing (all authors).

Conflicts of interest

There are no conflicts to declare.

Data availability

All relevant data that support these experimental findings are available from the corresponding author upon reasonable request.

Supplementary information (SI): a sample preparation schematic, additional calibration curves, and complete emission surveys. See DOI: **https://doi.org/10.1039/d5ja00319a**.

Acknowledgements

The work was funded by the State of Florida. This work was funded by the US Department of Energy's Office of Nuclear Energy, Advanced Reactor Development Program, Molten Salt Reactor Program.

References

1 D. LeBlanc, *Nucl. Eng. Des.*, 2010, **240**, 1644–1656.
2 J. Serp, M. Allibert, O. Beneš, S. Delpech, O. Feynberg, V. Ghetta, D. Heuer, D. Holcomb, V. Ignatiev and J. L. Kloosterman, *Prog. Nucl. Energy*, 2014, **77**, 308–319.
3 H. B. Andrews, J. McFarlane, A. S. Chapel, N. D. B. Ezell, D. E. Holcomb, D. de Wet, M. S. Greenwood, K. G. Myhre, S. A. Bryan and A. Lines, *Nucl. Eng. Des.*, 2021, **385**, 111529.
4 J. Moon, K. Myhre, H. Andrews and J. McFarlane, *Prog. Nucl. Energy*, 2022, **152**, 104369.
5 J. Moon, K. Myhre, H. Andrews and J. McFarlane, *Nucl. Technol.*, 2023, **209**, 787–808.
6 K. Shi, X. Hou, P. Roos and W. Wu, *Anal. Chim. Acta*, 2012, **709**, 1–20.
7 G. Desmet and C. Myttenaere, *Technetium in the Environment*, Springer Science & Business Media, 1986.
8 D. I. Kaplan and R. Jeffrey, *Radiochim. Acta*, 1998, **81**, 117–124.
9 K. H. Lieser, *Nuclear and Radiochemistry: Fundamentals and Applications*, John Wiley & Sons, 2008.
10 J. P. Icenhower, N. Qafoku, W. J. Martin and J. M. Zachara, *The Geochemistry of Technetium: a Summary of the Behavior of an Artificial Element in the Natural Environment*, Pacific Northwest National Lab.(PNNL), Richland, WA (United States), 2008.
11 I. Alliot, C. Alliot, P. Vitorge and M. Fattahi, *Environ. Sci. Technol.*, 2009, **43**, 9174–9182.
12 N. A. Wall, N. Karunathilake and W. Dong, *Radiochim. Acta*, 2013, **101**, 111–116.
13 Q. Chen, H. Dahlgaard, H. Hansen and A. Aarkrog, *Anal. Chim. Acta*, 1990, **228**, 163–167.
14 J. Chiu, T. Chu and P. Weng, *J. Radioanal. Nucl. Chem.*, 1991, **150**, 493–507.
15 D. Beals, *J. Radioanal. Nucl. Chem.*, 1996, **204**, 253–263.
16 R. Seki and M. Kondo, *J. Radioanal. Nucl. Chem.*, 2005, **263**, 393–398.
17 A. Eroglu, C. Mcleod and K. Leonard, *J. Anal. At. Spectrom.*, 1998, **13**, 875–878.
18 L. Wacker, L. K. Fifield and S. Tims, *Nucl. Instrum. Methods Phys. Res., Sect. B*, 2004, **223**, 185–189.
19 O. Egorov, M. J. O'Hara, J. Ruzicka and J. W. Grate, *Anal. Chem.*, 1998, **70**, 977–984.
20 E. H. Kwapis, J. Borrero, K. S. Latty, H. B. Andrews, S. S. Phongikaroon and K. C. Hartig, *Appl. Spectrosc.*, 2024, **78**, 9–55.
21 H. B. Andrews, Z. B. Kitzhaber, D. Orea and J. McFarlane, *J. Am. Chem. Soc.*, 2024, **147**, 910–917.
22 D. W. Hahn and N. Omenetto, *Appl. Spectrosc.*, 2012, **66**, 347–419.
23 A. K. Rai, F.-Y. Yueh and J. P. Singh, *Appl. Opt.*, 2003, **42**, 2078–2084.
24 V. N. Rai, F.-Y. Yueh and J. P. Singh, *Appl. Opt.*, 2003, **42**, 2094–2101.
25 F.-Y. Yueh, R. C. Sharma, J. P. Singh, H. Zhang and W. A. Spencer, *J. Air Waste Manage. Assoc.*, 2002, **52**, 1307–1315.
26 O. Samek, D. C. Beddows, J. Kaiser, S. V. Kukhlevsky, M. Liska, H. H. Telle and A. J. Whitehouse, *Opt. Eng.*, 2000, **39**, 2248–2262.
27 Q. Lin, X. Han, J. Wang, Z. Wei, K. Liu and Y. Duan, *J. Anal. At. Spectrom.*, 2016, **31**, 1622–1630.
28 W. Bozman, W. Meggers and C. Corliss, *J. Res. Natl. Bur. Stand., Sect. A*, 1967, **71**, 547.
29 Y. Ralchenko, *Memorie Della Società Astronomica Italiana Supplement*, 2005, vol. 8, p. 96.
30 J.-M. Mermet, *Spectrochim. Acta, Part B*, 2008, **63**, 166–182.
31 J.-M. Mermet, *Spectrochim. Acta, Part B*, 1994, **49**, 1313–1324.
32 H. B. Andrews, Z. B. Kitzhaber and J. McFarlane, *Spectrochim. Acta, Part B*, 2025, 107237.